RSC Sustainability

ROYAL SOCIETY OF CHEMISTRY

PAPER

View Article Online
View Journal | View Issue

Cite this: *RSC Sustainability*, 2023, **1**, 1200

Biochar as a substitute for graphite in microbial electrochemical technologies†

Sofía Antic Gorrazzi,[a] Diego Massazza,[a] Andrea Pedetta,[a] Leonel Silva,[b] Belén Prados,[c] Gastón Fouga[c] and Sebastián Bonanni *[a]

Biochar has emerged as an attractive electrode material due to its biocompatibility, low cost and reduced environmental impact. The temperature at which biochar is produced greatly affects its physicochemical properties and its environmental performance. Despite that, only biochar obtained at relatively high temperatures (800 to 1000 °C) has been applied in microbial electrochemical technologies (METs) so far. In this work, the physicochemical and electrical properties of biochar electrodes obtained at several temperatures (500 °C to 1000 °C) are explored and compared to those of graphite which is the most commonly used electrode material in METs. Besides, the associated carbon emissions and energy input of the production process at each temperature are estimated and compared to those of graphite. Results indicate that low-temperature (600 °C) biochar electrodes generate about half of the electric current obtained with high-temperature biochar or graphite electrodes. Furthermore, carbon emissions and energetic inputs for the production of low-temperature biochar are much lower than those of graphite production, with the 600 °C electrodes having a net positive carbon footprint and also a lower production cost. Nevertheless, further research is needed to optimize biochar conductivity and mechanical performance in order to allow its integration into large scale METs.

Received 29th January 2023
Accepted 19th May 2023

DOI: 10.1039/d3su00041a

rsc.li/rscsus

Sustainability spotlight

As stated in the UN's Sustainable Development Goals (SDG12 and SDG13) the application of sustainable patterns of production including the reduction of material footprint and greenhouse gas emissions is essential for mitigating climate change and lowering biodiversity loss and pollution. Electrochemical grade graphite production is based on the extraction of mineral ores and fossil fuels and is associated with high energy inputs and carbon emissions. In this work we study the use of biochar obtained from pruning residues as an alternative to graphite in bioelectrochemical systems showing that this material has an acceptable performance and, more importantly, requires low energy input for its production and can have a net positive carbon footprint.

Introduction

Electro-active microorganisms, such as the model bacterium *Geobacter sulfurreducens*, can use electrodes either as electron donors or acceptors generating an electric current directly associated with their metabolism.[1] They are applied in microbial electrochemical technologies (METs) where they catalyse redox reactions for wastewater treatment, bio-electrosynthesis or the production of energy carriers such as hydrogen and methane.

Electrode materials play a crucial role in MET performance and cost.[2] The high cost of the electrodes represents a major drawback of microbial electrochemical technologies and the identification of cheap materials is essential for allowing the scale-up and commercialization of METs.[3] Hence, the study and development of efficient and cost-effective electrodes is a very active research field.[4]

Graphite is the most widely used electrode material in METs due to its excellent electrochemical properties, biocompatibility, chemical stability and the variety of forms in which it is commercially available (rods, fibre brushes, granules, carbon-fibre cloths, paper sheets and felts, among others).[5]

Graphite is one of the crystalline forms of carbon and can be obtained either through mining of natural ores or through synthetic means.[6] Its content in the ore from which this material is obtained in nature varies between 5 and 40% by weight. In order to achieve the purity needed for electrochemical application, mechanical separation of graphite from the ore and chemical and/or thermal post-treatments are required.[6] On

[a]*División Ingeniería de Interfases y Bioprocesos (IIBio), INTEMA. Av. Colon 10850, Mar del Plata (7600), Argentina. E-mail: sebastian.bonanni@fi.mdp.edu.ar*

[b]*División Ciencia e Ingeniería de Polímeros, INTEMA. Av. Colon 10850, Mar del Plata (7600), Argentina*

[c]*Instituto de Energía y Desarrollo Sustentable, Centro Atómico Bariloche, CNEA, Av. E. Bustillo 9500, 8400 S. C. de Bariloche, Rio Negro, Argentina*

† Electronic supplementary information (ESI) available. See DOI: https://doi.org/10.1039/d3su00041a

the other hand, synthetic graphite is obtained commonly from petroleum coke or coal pitch, through a high energy demand process that, among several steps (calcination, crushing, baking, impregnation), involves heating unstructured carbons to temperatures above 2500 °C in order to generate a crystalline structure.

The non-renewable nature of the raw materials of both natural and synthetic graphite, as well as the high energy demand and associated carbon emissions of its manufacturing processes, makes graphite a non-sustainable electrode material. Furthermore, due to the complexity of the required equipment, electrochemical grade graphite has a high cost that may rise in the near future due to the increasing demand for its application in Li-ion batteries for electric vehicles. Alternative materials for replacing graphite with lower manufacturing costs, higher availability and lower environmental impact must thus be investigated.

Biochar has emerged as an attractive electroconductive and biocompatible material due to its low cost and reduced environmental impact. It is conventionally obtained by subjecting biomass to reductive pyrolysis, which consists in heating in an anoxic atmosphere. Feedstocks used for biochar production are diverse and include lignocellulosic matter such as wood chips and pellets, husks, and forestry and crop residues, as well as alternative biomass sources such as sewage sludge, poultry litter, dairy manure and bones.[7]

Besides allowing waste valorisation, biochar has a high carbon content of up to 90% by weight.[7] This carbon forms stable chemical structures that, according to recent estimations, may last between 90 and 1600 years in the material.[8] In this way, CO_2 emissions that would have been produced if biochar feedstocks were subjected to composting or incineration are avoided. Consequently, biochar production stands as an emerging carbon sequestration strategy.[9]

In addition, biochar is widely used as fuel for combustion,[10] as a soil amendment to improve crop yield[11,12] and as an adsorbent for the removal of contaminants from drinking water and wastewaters.[13] Recently, it has been applied in biological wastewater treatment systems such as anaerobic digesters[14,15] and treatment wetlands.[16–18] In such systems, biochar improves several aspects: it boosts microbial activity by allowing electron exchange between microbial species, it increases the buffer capacity of the liquid media and it can be used as a substrate for biofilm growth.

Recently, biochar has been applied as an electrode material in microbial electrochemical technologies.[5,19–21] As an electrode material, it has shown improved efficiency when compared with traditional graphite electrodes in terms of produced power,[22–24] projected current density[19,20,25] and volumetric current densities.[25] Biochar was also used as a base material for improving oxygen reduction on cathodes.[26]

The electric conductivity and the porosity of biochar, properties of great importance for its application in electrochemical systems, are strongly dependent on the temperature of pyrolysis, which usually ranges between 350 and 1000 °C.[7] Furthermore, the energy input, carbon emissions and production cost of the material as well as the complexity and cost of the equipment needed for its production are also highly dependent on the processing temperature. Despite this, only high temperatures ranging between 800 and 1000 °C have been used so far for obtaining biochar for MET electrodes.[27,28]

In this work, biochar electrodes of controlled area obtained at different temperatures with *Cyperus papyrus* as feedstock were used as electrode materials for the growth of electro-active bacteria. Compared to other macrophytes with similar characteristics, this species is commonly applied in treatment wetlands, requiring an annual pruning that generates large amounts of solid residues. The macrophytes' characteristic shape with elongated, cylindrical stems and a relatively uniform diameter along their length make them attractive for application as electrode materials allowing the revalorization of pruning residues.

The current produced by *Geobacter sulfurreducens* on biochar electrodes obtained at different temperatures was compared to that produced on graphite. It was found that more than half of the electric current obtained with graphite electrodes can be produced with low temperature biochar electrodes (600 °C). Furthermore, lowering the temperature of biochar production reduces both the associated energetic input and carbon emissions, with low temperature (600 °C) biochar having a net positive carbon footprint. Besides, cheaper equipment can be applied for obtaining biochar at low temperature, reducing the cost of the material.

Further research is needed to optimize biochar properties such as conductivity and mechanical performance to allow its integration into large scale METs. Nevertheless, due to the low cost and favourable environmental impact of low-temperature biochar this is an interesting challenge that may allow improvement in the applicability and sustainability of microbial electrochemical technologies.

Experimental

Biochar production

Papyrus (*Cyperus papyrus*) obtained from pruning residues of a treatment wetland was used as feedstock for biochar production. Stems were cut down to pieces of 2–3 cm and dehydrated at 105 °C for 24 hours. The resulting material was heated in a N_2 atmosphere at maximum temperatures of 500, 600, 800 and 1000 °C for 60 minutes with a heating rate of 10 °C min^{-1} in a tube furnace (Indef Model T-300). A cooling rate of 5 °C min^{-1} was maintained until a temperature of 25 °C was reached. Both heating rate and selected pyrolysis time are values typically used in the pyrolysis process.[27,29] Mass yield (%) was calculated from the weight lost in each pyrolysis process ($N = 2$).

Physicochemical characterisation

Relative quinone content. The chemical composition of the material produced at different temperatures was analyzed by Fourier Transform Infrared Spectroscopy (FT-IR) (Nicolet 6700, Thermo Scientific). To obtain a relative amount of quinones, a peak that did not vary with temperature was identified

($2160\ cm^{-1}$) and taken as a reference to standardize the area under the peak corresponding to quinones ($1590\ cm^{-1}$)[30] for each pyrolysis temperature. FT-IR spectra are shown in the ESI.†

Graphitization. Raman spectra were acquired in a Renishaw In-Via reflex system equipped with a charge-coupled device (CCD) detector of 1040 × 256 pixels. A 514 nm diode laser (50 mW) was used as an excitation source in combination with a grating of 2400 grooves per mm and slit openings of 65 μm, which yield a spectral resolution of about $4\ cm^{-1}$. The laser power was kept to 100%. A 50× (0.5 NA) long working distance (8 mm) Leica metallurgical objective was used in the excitation and collection paths. Spectra were typically acquired in 10 seconds with 5 accumulations. The fitting of the spectra was carried out using the Wire software v3.4 (Renishaw). Spectra were baseline subtracted using the cubic spline interpolation at specific Raman shifts. A fixed number of peaks were used in all the calculations. Peaks were fitted using a free combination of Lorentzian functions, as proposed in an earlier study.[31] Initial values for peak positions were taken as 1585, 1350, 1620, 1500 and 1200 cm^{-1} corresponding to peak G (ideal graphitic), D1 (disordered graphitic edges, in-plane imperfections), D2 (disordered graphitic surface), D3 (amorphous carbon, sp^2 bonded) and D4 (disordered graphite lattice, ionic impurities). A representative fitting is shown in the ESI.†

Mechanical strength. The vertical compressive resistance of biochar samples obtained at 800 °C ($N = 2$) and graphite rods ($N = 4$) was measured with a compression assay (EMIC 23 50 Instron Co., USA) at a crushing speed of 0.3 mm min^{-1}. The breaking load was recorded from the instrument, and compressive strength was calculated by breaking load and surface area.

Electric conductivity. The electric conductivity of graphite and biochar produced at different temperatures was measured with a 2-point cell. This cell was connected to a power source that allowed setting potential differences between the extremes of the material and measured the current flowing through it. When plotting current *vs.* potential difference, a straight line was obtained whose slope, according to Ohm's law, is the inverse of the resistance, known as conductance. This value multiplied by the length of the material and divided by its cross-sectional area gave the conductivity of the material. Measurements were performed in duplicate on the biochar produced at each temperature.

Zeta potential. The zeta potential of *G. sulfurreducens* and biochar samples was determined from the mean of 6 measurements (100 runs each) at 25 °C with a 633 nm laser (Zetasizer Nano ZS 90, Malvern). *G. sulfurreducens* cells were grown in vials at 30 °C with their typical growing medium using acetate as electron donor and fumarate as electron acceptor. After reaching an optical density of 0.4, the cells were centrifuged at 10 000 rpm for 20 min. The cell pellet was washed with PBS (pH 7.4) three times and resuspended in a dilution (1/10) of the same buffer. The cell suspension was vortexed before the zeta potential measurement was performed. The biochar samples were ground in a manual pulverizing mill in a tungsten carbide vessel (HSM, Herzog). Two cycles of 30 s each were performed. Then, the particle size distribution was analyzed by laser diffractometry (Cilas 1190 particle size analyzer) to confirm that particles with a size distribution smaller than 10 μm were obtained. The samples were resuspended in a high (100 mM) and a low (10 mM) salt solution (KNO_3), sonicated in a water bath for 20 minutes and stored for 24 h to stabilize their pH. The samples were sonicated again for 20 minutes and pH was measured (around 5.5 for each sample). pH was lowered with HNO_3 (pH 3) or increased with KOH (pH 13). ZP was measured immediately after pH adjustment. ZP is shown as the mean of three measurements (100 runs each). Three independent analyses were performed.

Chemical composition. The surface elemental composition of biochar and graphite was analyzed by X-ray photoelectron spectrometry (XPS, Thermo Scientific™ K-alpha+, USA) with an Al Kα X-ray source and a spot size of 300 μm. The pass energy for survey scans was 150 eV with a scan step of 1 eV. Following standard procedures,[32] carbon and oxygen contents were determined from the peak areas of C(1s) and O(1s) measured with Avantage software. The weight fraction of the biochar chemical elements was also determined by scanning electron microscopy with energy-dispersive X-ray spectroscopy (SEM-EDS). The ash content of biochar samples was quantified following a standard procedure.[33]

XRD. X-ray diffraction (XRD) patterns were recorded at room temperature on a BRUKER D8 Advance diffractometer with Bragg–Brentano θ/θ geometry and Cu Kα1 + Kα2 radiation (40 kV, 30 mA) in the 2θ range 5°–90° in steps of 0.02° and with a collection time of 2 s per step. Patterns were analyzed according to standard procedures.[34] The detected crystalline faces are listed in the ESI.†

Biochar electrodes as chemical electron acceptors. To analyze the use of the chemical components of biochar as electron acceptors supporting the growth of electro-active bacteria, vials of 3 g L^{-1} were inoculated with 3.07×10^5 cells per mL of a late exponential phase culture of *G. sulfurreducens*. Bacterial growth was followed through suspended cells quantification with a Neubauer chamber (Marienfeld). Biochar samples were analyzed with FTIR prior to and after bacterial growth to detect changes in their chemical composition. Results are shown in the ESI.†

Biochar anode material

Preparation of electrodes. Graphite rods were glued to biochar pieces of approximately 1 cm with an electro-conductive resin (AA-DUCT 906, ATOM adhesives). The potentiostat tip was connected to the graphite rod. To control the area exposed to the solution, these electrodes were included in epoxy resin. In this way only one transverse face of the biochar was exposed to the culture medium that was inoculated with the bacteria. Each electrode was then polished with 120 and 1000 grit sandpaper, until the exposed surface of the biochar was uniform. To remove loose particles from the surface, electrodes were sonicated for 1 min and rinsed with distilled water. Electric conductance between the graphite end and the biochar was checked by measuring the resistance between the two extremes of the electrode with a multimeter. Graphite rod electrodes ($d = 4$mm)

were used as reference working electrodes. These electrodes were also polished with 1000 grit sandpaper, sonicated for 1 min, and rinsed with distilled water.

From now on E500, E600, E800 and E1000 will be used to refer to electrodes obtained at 500, 600, 800 and 1000 °C, respectively.

Growth of electro-active bacteria and electrochemical analysis. The experimental system used to evaluate E500, E600, E800 and E1000 as working electrode materials was a single chamber three electrode electrochemical cell adapted for the growth of anaerobic electro-active microorganisms. An inoculum of *G. sulfurreducens* strain DSM12127 was first anaerobically grown in batches at 30 °C on a medium prepared as described in an earlier study[35] that contained acetate (20 mM) as electron donor and fumarate (40 mM) as electron acceptor. For electrogenic growth, this batch culture at an early stationary phase was inoculated into the cell (1×10^6–1×10^7 bacteria per cm^3 as final concentration) that contained deoxygenated culture medium with acetate (20 mM) and no fumarate. The culture medium was circulated by the electrochemical cell using PharMed tubing and a low-rate peristaltic pump. The pH of the medium was kept constant at a value of 7.3 by bubbling all media reservoirs and the reactor with a mixture of N_2/CO_2 (80 : 20). The cell was polarized at a constant potential of 0.2 V *vs.* an Ag/AgCl (3 M NaCl) reference electrode by using a Pt wire as a counter electrode. All electrochemical assays were performed by using an AUTOLAB PGSTAT101 potentiostat controlled by 2.1 NOVA dedicated software.

The stable current density (j) of each working electrode was calculated from the individual current of each electrode divided by their arithmetic area. For the biochar electrodes, the area measurements were performed with ImageJ software.

The values of current density from each electrogenic culture assay included in a range of ±SD ($N = 4$ for E600 and graphite and $N = 3$ for the others) were statistically analyzed. Normality of the data set was analyzed using the Shapiro–Wilk test. After confirming normality, Fisher's F-test was performed to analyze the homoscedasticity of the samples and two-tailed Student's t-test. The significance level was 0.05 (p-value).

SEM observation of the electrodes. Graphite rods and biochar electrodes with and without biofilm on their surface were observed. Microscopic observation of the material's internal structure was performed and pore sizes were measured on randomly chosen spots. For biofilm observation, once the electrical current generated by bacteria was stable, electrodes were removed from the cell and fixed with glutaraldehyde 2.5% for 2.5 hours and dehydrated on sequential solutions of ethyl alcohol (30, 40, 60, 80 and 100%) for 15 minutes. Prior to its observation, the samples were metalized with gold following standard procedures.

Biomass quantification on electrodes. Biofilms from biochar and graphite electrodes were removed and genomic DNA was extracted for each electrode with the phenol–chloroform method in duplicate.

The integrity of the extracted DNA was checked by electrophoresis on a 1.2% agarose gel. DNA quantification (ng DNA per µl of sample) was analyzed with a NanoDrop spectrophotometer. Since low-temperature biochar can interfere with DNA quantification because of the presence of functional groups on its surface,[36] DNA quantification of E500 and E600 electrodes was performed directly from the gel using ImageJ software. The ratio between the concentration obtained from the gel for the biochar and graphite electrodes was multiplied by the concentration measured for graphite electrodes with the Nanodrop spectrophotometer to calculate the DNA concentration in E500 and E600 samples. The number of bacteria (NB) was obtained from the DNA content of a single bacterium determined by quantification of total DNA from samples of known bacteria density (1×10^7 cells per μg_{DNA}).

Results and discussion

Biochar composition

Electro-active bacteria grow forming biofilms that are tens of micrometres thick using an anode as electron acceptor and generating in this way an electric current directly coupled with its metabolic activity. Several variables influence the formation of the electro-active biofilm and its current production efficiency. The chemical composition of the electrode material and its surface crystallography are aspects of great importance for the biofilm formation process, as they have a strong influence on the forces acting during the initial steps of bacterial adhesion and the efficiency of the electron transfer between the bacteria and the electrode.[37,38] Besides, the conductivity of the electrode plays a crucial role in the current production process. It determines the electrochemical potential sensed by the bacteria on the electrode surface, which has a great influence on the rate of electron transfer from the cells to the electrode.

Several changes in biochar composition, structure and conductivity occur with increasing pyrolysis temperature.[39] Consequently, variations in electric current production are expected among biochar electrodes obtained at different temperatures.

During pyrolysis, the feedstock is subjected to a complex set of chemical reactions that include the condensation of aliphatic and aromatic compounds in conjugated structures and the release of volatile molecules (alcohols, oils, tar), methane, carbon monoxide and hydrogen.[40] The extent to which these reactions proceed is largely determined by the temperature of the heat treatment process.[41] At relatively low temperatures (between 300 and 600 °C) liquid and tar forming reactions prevail. At temperatures above 600 °C the removal of oxygen, nitrogen and sulfur as well as condensation reactions becomes increasingly important. Consequently, the oxygen content of biochar samples decreased with pyrolysis temperature (see ESI†).

Among the oxygenated chemical compounds of biochar, quinone-like compounds are one of the most prevalent.[42] These components have C=O bonds that, being formed by atoms of different electronegativity, generate regions of differential charge density on its structure. In accordance with the decay in oxygen content, FTIR assays showed a decrease in the concentration of quinone-like components with increasing pyrolysis temperature (see ESI†).

In contrast to oxygen, the carbon content of biochar increased with pyrolysis temperature. This occurs because during condensation reactions (that become increasingly important at higher temperatures) carbon becomes part of the stable and highly conjugated aromatic compounds. In these compounds, the carbon atoms form a local crystalline structure resembling that of graphite, with stacked flat aromatic sheets that are randomly cross-linked.[43]

Biochar also has inorganic moieties. The inorganic fraction of biochar electrodes was mainly formed by sodium, potassium, calcium and magnesium salts that, according to elemental analysis, showed increasing content with pyrolysis temperature (see ESI†), as previously reported.[12] The ash content of E1000 biochar was 12.4 ± 0.7%, whereas the ash content of the feedstock was 6.0 ± 0.5%. No ash was obtained on graphite samples. The results of TGA in an oxygen atmosphere for graphite and E1000 are shown in the ESI.† Salts were detected only in raw biochar samples and not in samples used as electrodes in electrochemical cells, most likely due to their solubilization in the liquid media.

Despite the observed changes in biochar composition, the zeta potential which is used as an indirect measure of the surface charge of particles[44] was similar for all samples (see ESI†), suggesting the existence of similar charge densities on the surface of the electrodes.

Structure and mechanical strength

Biochar produced from plant stems shows the vascular morphology of the precursor plant.[1,25] The feedstock used in this work, *Cyperus papyrus*, has a triangular stem with numerous intercellular spaces forming large longitudinal pores (see ESI†). These cavities are straight and continuous along the stem and their diameter does not vary significantly from the base to the top. Immersed in this structure, the plant also has vascular bundles that form randomly arranged pores of smaller size. All these cavities are disposed continuously throughout the plant stem, shaping the internal structure of the biochar which is dominated with pores of different diameters. Pyrolysis temperature did not modify the internal structure nor the size of pores which ranged between 3 and 130 μm in all cases (see ESI†).

The increased molecular order of the pyrolyzed biomass gives it a higher mechanical strength than the feedstock from which it was derived.[43] Despite this, the biochar produced in this work had similar mechanical strength at all temperatures. Mean resistance to compression was 0.63 ± 0.08 MPa, which is much lower than that of graphite (4.70 ± 0.71 MPa). Strategies such as densification of the obtained biochar with pyrolysis oil or other binders,[45] or the selection of harder feedstocks such as those with high lignin content, may be plausible alternatives to increase biochar's mechanical strength and to improve its applicability of biochar electrodes on large scale systems.

Current production

The biochar samples obtained at different temperatures were polarized at 0.2 V (*vs.* Ag/AgCl) on electrochemical cells inoculated with *G. sulfurreducens*. The increase of current density produced by the electrodes just after inoculation can be used to analyse the initial colonization of the electrodes,[37] which was similar in all cases (data not shown). This suggests that the initial adherence efficiency did not vary between the materials, in accordance with similar charge densities estimated through zeta potential. Nevertheless, once the biofilms fully developed, the final electric current density produced by the electro-active biofilms on the biochar electrodes strongly depended on the pyrolysis temperature of the electrode.

Chemical compounds in low-temperature biochar (*e.g.* quinones) may serve as electron acceptors for electro-active bacteria (see ESI†).[46] Nevertheless, the electric current obtained with E500 electrodes was very similar to the current prior to inoculation (blank), indicating that little or no bacterial growth was caused by these electrodes.

The E800 and E1000 current density values were similar to those of graphite electrodes, whereas intermediate current densities were obtained with E600 electrodes (Fig. 1A).

The differences in obtained current densities are explained by structural changes promoted by high pyrolysis temperatures. Graphitization was analysed by Raman micro-spectroscopy (see ESI†). Raman spectra suggest that E500 was formed mainly by amorphous (disordered) carbon, whereas higher temperature

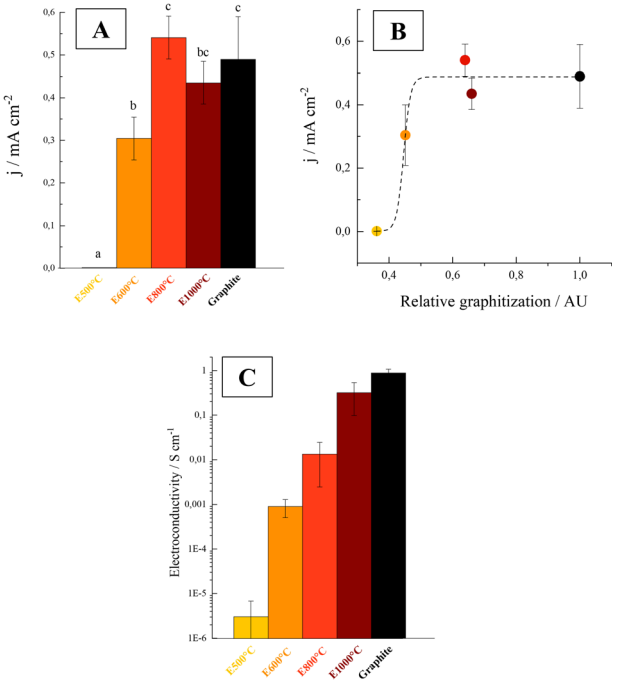

Fig. 1 (A) Electric current density (*j*) produced on E500 (yellow), E600 (orange), E800 (red), E1000 (dark red) and graphite (black) electrodes by *G. sulfurreducens* cells. Base currents were subtracted. Letters on the bars indicate statistically significant differences between electrodes ($p < 0.05$). $N = 4$ for graphite and $N = 3$ for the other electrodes. (B) Electric current density (*j*) as a function of relative graphitization (calculated as the ratio between G and G + D peak areas of the Raman spectra, see ESI† for details) for biochar electrodes and graphite. The dotted line represents the fitting with an asymptotic function. (C) Electroconductivity (S cm^{-1}) of different biochar and graphite electrodes ($N = 2$).

biochar showed a progressive decrease in the disorder and an increase in the degree of graphitization, as previously reported for other feedstocks.[47–49]

The current density produced by the bacteria highly depended on the degree of graphitization of the electrodes (estimated here from the fraction of total peak area represented by graphitic peak G, see ESI†). These two variables showed an asymptotic relation (Fig. 1B). In this context, the graphitization degree may be a useful parameter to preliminarily determine whether the biochar obtained from different feedstocks and under different pyrolysis conditions could be used as an electrode material for electro-active bacteria growth.

Graphite crystallites are formed by organized clusters of sp^2 hybridized atoms. As the π electrons of sp^2 carbons are responsible for the electrical conductivity of biochar, the graphitization degree highly influences the conductivity of the material.[49] As a result of the higher degrees of graphitization shown above, higher conductivities were obtained with increasing pyrolysis temperatures (Fig. 1C). The conductivity of the material exhibited a significant increase when the pyrolysis temperature was raised from 500 to 600 °C. At higher temperatures, a progressive enhancement in conductivity was observed, with the materials pyrolyzed at 1000 °C having conductivities within the same order of magnitude as that of graphite.

Electrode conductivity is of great importance for MET efficiency as it determines the potential sensed by the bacteria at the electrode/solution interface. When growing bacteria on three-electrode cells as those used in this work, a potential is applied at one end of the working electrode with a potentiostat, but the actual potential at the face of the electrode submerged on the liquid media may differ from the applied value, since the electron flow through the electrode generates a potential drop. Consequently, if the electrode is not sufficiently conductive, the real potential may not be favourable for bacterial respiration, interfering with the generation of electric current.

Taking the mean produced current densities at each electrode and the respective electric conductivities, potential drops across the biochar material of 350 mV, 40 mV and 0.4 mV were estimated for E600, E800 and E1000 respectively. As the applied potential to the working electrode was 0.2 V *vs.* Ag/AgCl, it can be estimated that the actual potential at the electrode/biofilm interface was −150 mV, 260 mV and 199 mV *vs.* Ag/AgCl for each of these electrodes. Considering that the lowest potential value at which *G. sulfurreducens* can use an anode as electron acceptor is around −0.45 V *vs.* Ag/AgCl, these values indicate that the actual potential applied to the electrodes was favourable for bacterial respiration in all cases.

On the other hand, a much higher potential drop was estimated for the E500 electrodes (close to 1.2 V). This indicates that the real potential on the submerged face of the E500 electrodes was unfavourable for bacterial respiration, and that the low amount of current obtained on these electrodes was not related to bacterial respiration.

To gain further insight into the relationship between current and applied potential, cyclic voltammetry was performed (Fig. 2). In accordance with the higher conductivity of the

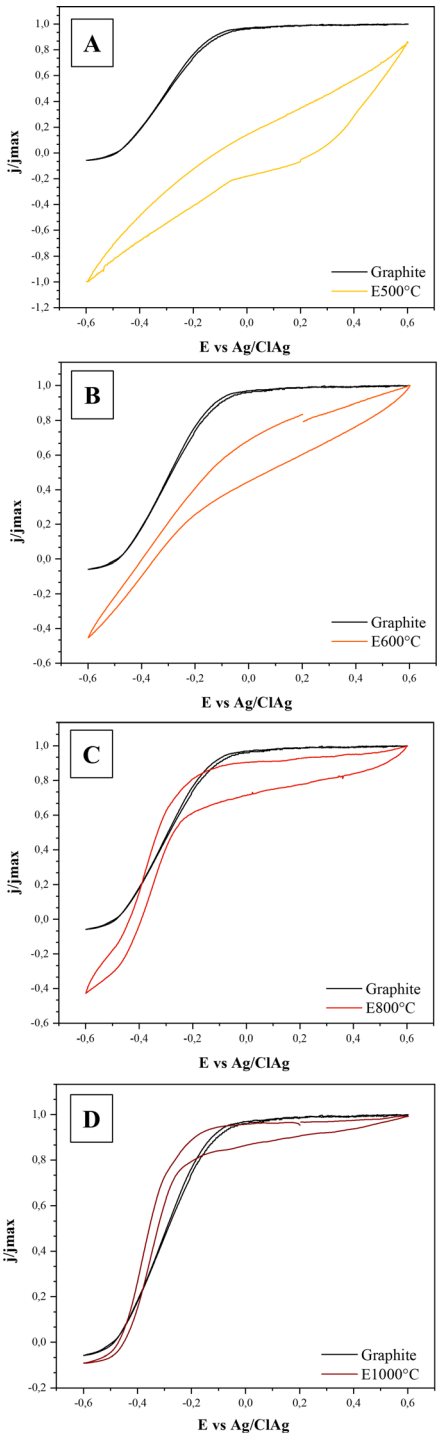

Fig. 2 Comparison between voltammograms of graphite (black line) and biochar electrodes obtained at different temperatures: 500 °C (A), 600 °C (B), 800 °C (C), and 1000 °C (D) in a single chamber three electrode electrochemical cell with *G. sulfurreducens* already grown. Cyclic voltammetry was performed at 0.001 V s^{-1} and current density divided by maximal current density (j/j_{max}) *vs.* potential (E/V) is plotted in the y axis.

electrodes, the CV signals of the E800 and E1000 electrodes were similar to that obtained with graphite.

In these cases, electric current production started at potentials of around −0.45 V *vs.* Ag/AgCl and showed a sustained

increase with the applied potential. This current increase is produced by an acceleration of bacterial metabolism due to the increasing oxidation of redox intermediates acting between the bacteria and the electrode.[50] Once a potential of around −0.2 to −0.1 V *vs.* Ag/AgCl was applied, cells were working at the maximum rate and electric current reached a stable value.

Signals of E600 showed a different behaviour, not reaching a stable current value even at the highest applied potential. As shown above, E600 electrodes had a lower (and possibly heterogeneous) conductivity than E800 and E1000 and, consequently, there may have existed areas where the actual electrode potential was below the values needed for optimal bacterial activity. In this context, despite allowing the production of a relatively high current density on the three-electrode cell configuration used in this work where the electrode length was small (~1 cm), the relatively low conductivity of the E600 electrode may preclude its application in systems where electrons have to be transported across longer distances, such as large-scale microbial fuel cells and microbial electrolysis cells. In fact, for these systems it has been stated that even graphite electrodes lack the appropriate conductivity for avoiding considerable ohmic drops. The application of current collectors was identified as a crucial design aspect for reducing ohmic drops and allowing an efficient scale up.[51] They would necessarily have to be applied when using biochar electrodes.

Cell density

From DNA extraction and quantification, it was estimated that bacterial density on E600 was $2.3 \pm 6.5 \times 10^9$ cells per cm^2, which is very similar to values of $2.9 \pm 0.5 \times 10^9$ and $2.0 \pm 0.9 \times 10^9$ found for the E1000 and graphite controls. On the other hand, considering the produced current densities and the bacterial densities on each electrode, it can be estimated that the mean respiration rate was 0.13 ± 0.01 pA per cell on E600 electrodes, whereas a value of 0.21 ± 0.05 pA can be estimated for graphite electrodes. This suggests that despite allowing the growth of similar number of bacteria, the low conductivity of E600 may have limited the respiration rate of the bacteria.

SEM images show that bacteria did not colonize the internal pores of the material (see ESI†) and were only found on the surface of the electrode, where they formed thick biofilms that covered even the larger pores of the material (Fig. 3). Nevertheless, the coverage of the 600 °C electrodes was not as homogeneous as that of the graphite electrodes. On those electrodes, biofilms had heterogeneous thickness, with some regions being covered by less than a monolayer (Fig. 3(D1)). This suggests that some parts were not favorable for electrode respiration by the bacteria, possibly due to particularly unfavorable potentials produced by heterogeneities in the conductivity of the electrode and/or the composition of the biochar. These heterogeneities may have reduced the current generated by the bacteria on certain portions of the electrode, explaining the lower respiration rate estimated above for these electrodes.

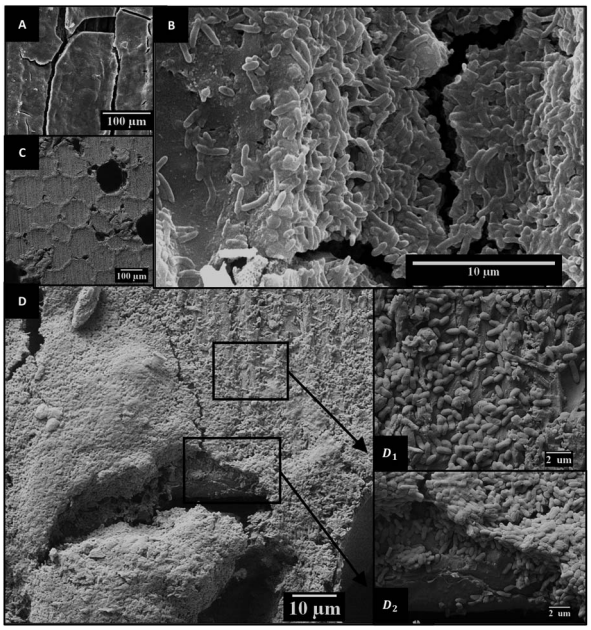

Fig. 3 SEM images of *G. sulfurreducens* biofilms grown on 1000 (A and C) and 600 °C biochar (B and D). Magnification of 1000 and 600 °C electrode micrographs (C and D1 and D2, respectively) clearly shows bacteria forming dense biofilms on both biochar electrodes. Nevertheless, the coverage of the surface is heterogeneous (D1 *vs.* D2).

Cost and sustainability

As shown in previous sections, biochar electrodes have similar efficiency to graphite for electric current production with electro-active bacteria. Due to the lower temperature of the thermal process required for its production, biochar electrodes are also a more economical and sustainable option than graphite.

Natural graphite is mined in open and underground pits and ore has low graphitic carbon content (2 to 30% by weight). In order to achieve the high purity (>99%) needed for its application in electrochemical devices, several beneficiation steps are required, including milling, flotation, leaching, roasting and thermal processing. Most of the energy demand of these processes is delivered from the combustion of fossil fuels, with the remaining 20 to 25% coming from electricity.[52]

Graphite can also be synthetically produced through what is known as the Acheson process. The most common feedstock for this process is coke, a solid material with high carbon content that derives from oil refining and cracking of heavy oils. To obtain graphite, coke must be calcined to remove volatile compounds and then subjected to a graphitization step that involves heating to temperatures above 2500 °C for about 3 to 5 days, commonly in electrically heated furnaces.

Further processing steps may involve grinding, impregnation with a binder and baking at temperatures between 800 and 1500 °C.

Consequently, the production of electrodes from both synthetic and natural graphite is energy intensive.[52] The estimated energetic input for natural graphite production ranges between 43.8 MJ kg^{-1} (ref. 53) to 112.48 MJ kg^{-1} (ref. 54) whereas the synthetic graphitization process has an estimated input of 45.9 MJ kg^{-1} (ref. 52).

Much lower energy is required to produce biochar through pyrolysis. Traditionally, biochar is applied as a soil amendment or for bioenergy production through combustion. For these applications, biochar is commonly obtained at temperatures ranging between 350 and 500 °C. As pyrolysis is an exothermic process and releases gases that can be combusted, a small amount of energy which is estimated to be 0.058 MJ kg^{-1} is only needed during initial start-up of the pyrolysis kiln.[55]

The production of biochar for its application as an electrode material is different from the traditional approach, as higher temperatures are required. Anyway, as will be shown, the energy requirement of the process is still much lower than that of graphite production. An estimation of the energy requirement of the pyrolysis will be performed by considering the production of biochar in an electric industrial oven. A heating ramp of 10 °C min^{-1} (like that applied in this work), an initial temperature of 20 °C and a pyrolysis time (at final temperature) of 60 min are considered. Also, the energy demand of a static chamber furnace that can handle 1.5 m^3 (750 kg of bulk material) per batch is considered (96 kW for Carbolite SBCF-3/11/1700). Considering these values and taking a mass yield of 30% like that obtained in this work (see ESI†), an energy demand of 3.0, 3.53 and 4.05 MJ kg^{-1} can be estimated for pyrolysis temperatures of 600, 800 and 1000 °C respectively.

Other steps in biochar manufacturing rather than pyrolysis also consume energy, with drying being the most important when using vegetables residues as feedstock. Depending on the feedstock and its initial water content, these steps can consume from 0.35 to 2.45 MJ kg^{-1}.[56] Taking the mean between these values together with the estimations for the pyrolysis process, the total energetic input for obtaining electrodes at 600, 800 and 1000 °C from vegetable residues can be estimated to be 4.40, 4.93 and 5.45 MJ kg^{-1} which are an order of magnitude lower than the estimations for graphite production. It has to be taken into account that if plants cultivated with the sole purpose of being used for biochar production are used as feedstock instead of vegetable residues, other energy demanding concepts should be considered in the process, such as the production of agrochemicals needed for plant growth and harvesting operations, which may account for up to 1.1 MJ kg^{-1} additionally.[56]

A low energetic demand is related to lower CO_2 emissions into the atmosphere, especially if the required energy is generated through fuel combustion. Taking as a reference the mean emissions of USA's electric energy grid, 0.57 kg CO_2 per kW h,[57] it can be estimated that emissions of the pyrolysis process are about 0.48, 0.56 and 0.64 kg CO_2 per kg for E600, E800 and E1000. Other sources of CO_2 emissions on the biochar production process are the production of agrochemicals, field operations and changes in land use related to feedstock cultivation, which together can be between 0.08 and 1.03 kg CO_2 per kg.[56] As previously mentioned, these latter emissions can be neglected if vegetable residues are used as feedstock.

Furthermore, it has to be considered that most carbon in biochar is in a highly stable state and, as a consequence, biochar can be used for carbon sequestration. As the carbon content of biochar obtained from plants and wood is about 70% by weight[7] and 80% of carbon in biochar is in stable form,[56] it can be estimated that biochar's carbon sequestering capacity is about 0.56 kg CO_2 per kg.

Notably, this estimation and the emissions estimated above suggest that E600 electrodes may have a positive carbon footprint of about 0.08 kg CO_2 per kg. This represents a great advantage of E600 electrodes in comparison with those obtained at higher temperatures and specially with graphite, a material whose production is related to high carbon emissions into the atmosphere ranging between 2.15 (ref. 53) and 5.3 kg CO_2 (ref. 54) per kg of graphite for the production of electrodes from natural graphite and reaching 13.8 kg CO_2 per kg of graphite (ref. 13 and 52) for its synthetic production.

Besides affecting the energy input and net carbon emissions, pyrolysis temperature also affects the cost of the equipment needed for the thermal treatment. Special nickel based alloys are needed for processes at high temperatures, whereas iron based materials and aluminium alloys can be used for lower temperatures up to 600 °C. Nickel based alloys are much more expensive than iron and aluminium and, as a consequence, high temperature ovens are much more expensive than low temperature ones that can be constructed with iron based materials such as stainless steel.[58] Estimations show that the equipment for achieving temperatures close to 1000 °C is almost 6 times more expensive than that for achieving temperatures lower than 650 °C.[59] Considering the cost of the energy and the depreciation of the equipment needed for biochar production, it was estimated that the cost for obtaining biochar at 600 °C is three times lower than for the production at 1000 °C.[60]

Conclusions

The use of biochar as an electrode material holds great promise for enhancing the sustainability and efficiency of METs and other electrochemical technologies. Low-temperature biochar can be a sustainable and cost-effective alternative to graphite as the electrode material in microbial electrochemical technologies, helping to address the current limitations of METs in this regard. The temperature applied during the pyrolysis process has a great influence on the properties of the material and consequently on the obtained current density, but also on carbon emissions related to the production process and the associated production cost. Higher temperatures favour graphitization thus increasing the conductivity and electric current production, but are also related to higher energetic demand, CO_2 emissions and cost increase of the equipment needed for material production. Similar electric current densities to those obtained with graphite can be obtained with biochar obtained at 800 to 1000 °C as electrode material. The current density obtained with biochar produced at 600 °C was more than half of that obtained with higher temperature biochar. Besides, the production of electrodes at this temperature will require lower cost equipment and a lower energy input and, most importantly, may be associated with a positive carbon footprint. This highly contrasts with the high cost, carbon emissions and energy inputs related to graphite electrode production. Consequently, biochar electrodes obtained at low

temperature may be a sustainable and cost-effective material for substituting graphite electrodes in bioelectrochemical systems.

Biochar electrodes still have some limitations that have to be overcome to allow their effective application. The low conductivity is a major drawback of biochar electrodes as the material, even when obtained at high temperatures, still lacks the needed electrical conductivity to allow electron transfer over long distances. Consequently, as noted previously for graphite electrodes, biochar electrode designs may have to incorporate metals as current collectors to allow their application in large scale systems. Obtaining higher conductivity electrodes at low pyrolysis temperature is a major challenge that may be addressed through the study of different feedstocks and the analysis of different pre-treatments.

Also, the mechanical strength of biochar must be improved for enhancing the applicability of biochar electrodes. Strategies such as densification with pyrolysis oil or other binders and the use of alternative feedstock with improved mechanical properties may be plausible strategies to achieve such improvement.

Author contributions

AGS: investigation, validation, data curation, formal analysis, visualisation and writing (review and editing). DM: funding acquisition, methodology, investigation, validation and writing (review and editing). PA: methodology, validation, and writing (review and editing). SL: methodology, data curation and validation (Raman assays). PB: methodology, validation and data curation (zeta potential assays). FG: methodology, validation and data curation (XRD and TGA assays). SB: conceptualization, funding acquisition, investigation, project administration, methodology, supervision and writing (original draft).

Conflicts of interest

There are no conflicts to declare.

Acknowledgements

This work was funded by ANPCyT PICT grant number 2019-2446. The assistance of Juan Pablo Busalmen, Rodrigo Parra, Hernan Romeo, Carlos Rodriguez Simón, Alejandro Robledo, Mariano Prudente and Andres Torres from INTEMA is acknowledged. AGS is a doctoral research fellow of CONICET (Argentina).

Notes and references

1 A. Schievano, R. Berenguer, A. Goglio, S. Bocchi, S. Marzorati, L. Rago, *et al.*, Electroactive biochar for large-scale environmental applications of microbial electrochemistry, *ACS Sustainable Chem. Eng.*, 2019, **7**(22), 18198–18212.

2 Y. Zhang and I. Angelidaki, Microbial Electrochemical Systems and Technologies: It Is Time To Report the Capital Costs, *Environ. Sci. Technol.*, 2016, **50**(11), 5432–5433.

3 D. A. Jadhav, S. G. Park, S. Pandit, E. Yang, M. Ali Abdelkareem, J. K. Jang, *et al.*, Scalability of microbial electrochemical technologies: Applications and challenges, *Bioresour. Technol.*, 2022, **345**, 126498.

4 A. A. Mier, H. Olvera-Vargas, M. Mejía-López, A. Longoria, L. Verea, P. J. Sebastian, *et al.*, A review of recent advances in electrode materials for emerging bioelectrochemical systems: From biofilm-bearing anodes to specialized cathodes, *Chemosphere*, 2021, **283**, 131138.

5 A. A. Yaqoob, M. N. M. Ibrahim and S. Rodríguez-Couto, Development and modification of materials to build cost-effective anodes for microbial fuel cells (MFCs): An overview, *Biochem. Eng. J.*, 2020, **164**, 107779.

6 M. Wissler, Graphite and carbon powders for electrochemical applications, *J. Power Sources*, 2006, **156**(2), 142–150.

7 A. Tomczyk, Z. Sokołowska and P. Boguta, Biochar physicochemical properties: pyrolysis temperature and feedstock kind effects, *Rev. Environ. Sci. Biotechnol.*, 2020, **19**(1), 191–215.

8 B. P. Singh, A. L. Cowie and R. J. Smernik, Biochar carbon stability in a clayey soil as a function of feedstock and pyrolysis temperature, *Environ. Sci. Technol.*, 2012, **46**(21), 11770–11778.

9 X. Cui, J. Wang, X. Wang, M. B. Khan, M. Lu, K. Y. Khan, *et al.*, Biochar from constructed wetland biomass waste: A review of its potential and challenges, *Chemosphere*, 2022, **287**, 132259.

10 Z. Liu and G. Han, Production of solid fuel biochar from waste biomass by low temperature pyrolysis, *Fuel*, 2015, **158**, 159–165.

11 K. Y. Chan, L. V. Zwieten, I. Meszaros, A. Downie, S. Joseph, K. Y. Chan, *et al.*, Agronomic values of greenwaste biochar as a soil amendment, *Soil Res.*, 2007, **45**(8), 629–634.

12 B. Singh, B. P. Singh, A. L. Cowie, B. Singh, B. P. Singh and A. L. Cowie, Characterisation and evaluation of biochars for their application as a soil amendment, *Soil Res.*, 2010, **48**(7), 516–525.

13 Q. Dai, J. C. Kelly, L. Gaines and M. Wang, Life cycle analysis of lithium-ion batteries for automotive applications, *Batteries*, 2019, **5**(2), 48.

14 J. Pan, J. Ma, L. Zhai, T. Luo, Z. Mei and H. Liu, Achievements of biochar application for enhanced anaerobic digestion: A review, *Bioresour. Technol.*, 2019, **292**, 122058.

15 W. Zhao, H. Yang, S. He, Q. Zhao and L. Wei, A review of biochar in anaerobic digestion to improve biogas production: Performances, mechanisms and economic assessments, *Bioresour. Technol.*, 2021, **341**, 125797.

16 A. Aguirre-Sierra, T. Bacchetti-De Gregoris, A. Berná, J. J. Salas, C. Aragón and A. Esteve-Núñez, Microbial electrochemical systems outperform fixed-bed biofilters in cleaning up urban wastewater, *Environ. Sci.: Water Res. Technol.*, 2016, **2**(6), 984–993.

17 A. Prado, C. A. Ramírez-Vargas, C. A. Arias and A. Esteve-Núñez, Novel bioelectrochemical strategies for

domesticating the electron flow in constructed wetlands, *Sci. Total Environ.*, 2020, **735**, 139522.
18 A. Prado de Nicolás, R. Berenguer and A. Esteve-Núñez, Evaluating bioelectrochemically-assisted constructed wetland (METland®) for treating wastewater: Analysis of materials, performance and electroactive communities, *Chem. Eng. J.*, 2022, **440**, 135748.
19 S. Chen, G. He, Q. Liu, F. Harnisch, Y. Zhou, Y. Chen, *et al.*, Layered corrugated electrode macrostructures boost microbial bioelectrocatalysis, *Energy Environ. Sci.*, 2012, **5**(12), 9769–9772.
20 R. Karthikeyan, B. Wang, J. Xuan, J. W. C. Wong, P. K. H. Lee and M. K. H. Leung, Interfacial electron transfer and bioelectrocatalysis of carbonized plant material as effective anode of microbial fuel cell, *Electrochim. Acta*, 2015, **157**, 314–323.
21 S. Chen, G. He, X. Hu, M. Xie, S. Wang, D. Zeng, *et al.*, A three-dimensionally ordered macroporous carbon derived from a natural resource as anode for microbial bioelectrochemical systems, *ChemSusChem*, 2012, **5**(6), 1059–1063.
22 T. Huggins, H. Wang, J. Kearns, P. Jenkins and Z. J. Ren, Biochar as a sustainable electrode material for electricity production in microbial fuel cells, *Bioresour. Technol.*, 2014, **157**, 114–119.
23 K. Senthilkumar and M. Naveenkumar, Enhanced performance study of microbial fuel cell using waste biomass-derived carbon electrode, *Biomass Convers. Biorefin.*, 2023, **13**, 5921–5929.
24 J. Zhang, J. Li, D. Ye, X. Zhu, Q. Liao and B. Zhang, Tubular bamboo charcoal for anode in microbial fuel cells, *J. Power Sources*, 2014, **272**, 277–282.
25 S. Chen, Q. Liu, G. He, Y. Zhou, M. Hanif, X. Peng, *et al.*, Reticulated carbon foam derived from a sponge-like natural product as a high-performance anode in microbial fuel cells, *J. Mater. Chem.*, 2012, **22**(35), 18609–18613.
26 S. Li, S. H. Ho, T. Hua, Q. Zhou, F. Li and J. Tang, Sustainable biochar as an electrocatalysts for the oxygen reduction reaction in microbial fuel cells, *Green Energy Environ.*, 2021, **6**(5), 644–659.
27 I. Chakraborty, S. Sathe, B. Dubey and M. Ghangrekar, Waste-derived biochar: applications and future perspective in microbial fuel cells, *Bioresour. Technol.*, 2020, **312**, 123587.
28 S. B. Patwardhan, S. Pandit, P. K. Gupta, N. K. Jha, J. Rawat, H. C. Joshi, *et al.*, Recent advances in the application of biochar in microbial electrochemical cells, *Fuel*, 2021, 122501.
29 M. Tripathi, J. N. Sahu and P. Ganesan, Effect of process parameters on production of biochar from biomass waste through pyrolysis: A review, *Renewable Sustainable Energy Rev.*, 2016, **55**, 467–481.
30 S. Kloss, F. Zehetner, A. Dellantonio, R. Hamid, F. Ottner, V. Liedtke, *et al.*, Characterization of slow pyrolysis biochars: effects of feedstocks and pyrolysis temperature on biochar properties, *J. Environ. Qual.*, 2012, **41**(4), 990–1000.
31 C. Sheng, Char structure characterised by Raman spectroscopy and its correlations with combustion reactivity, *Fuel*, 2007, **86**(15), 2316–2324.
32 B. Singh, Y. Fang, B. C. Cowie and L. Thomsen, NEXAFS and XPS characterisation of carbon functional groups of fresh and aged biochars, *Org. Geochem.*, 2014, **77**, 1–10.
33 A. Sluiter, B. Hames, R. Ruiz, C. Scarlata, J. Sluiter and D. Templeton, *Determination of Ash in Biomass (NREL/TP-510-42622)*, Natl Renew Energy Lab Gold, 2005, vol. 19.
34 File PD. Joint Committee on Powder Diffraction Standards, International Centre for Diffraction Data, Newton Sq PA Card, 1987, pp. 25–1280.
35 G. D. Schrott, P. S. Bonanni, L. Robuschi, A. Esteve-Nuñez and J. P. Busalmen, Electrochemical insight into the mechanism of electron transport in biofilms of Geobacter sulfurreducens, *Electrochim. Acta*, 2011, **56**(28), 10791–10795.
36 L. Hale and D. Crowley, DNA extraction methodology for biochar-amended sand and clay, *Biol. Fertil. Soils*, 2015, **51**(6), 733–738.
37 B. Maestro, J. M. Ortiz, G. Schrott, J. P. Busalmen, V. Climent and J. M. Feliu, Crystallographic orientation and electrode nature are key factors for electric current generation by Geobacter sulfurreducens, *Bioelectrochemistry*, 2014, **98**, 11–19.
38 M. Zhou, M. Chi, J. Luo, H. He and T. Jin, An overview of electrode materials in microbial fuel cells, *J. Power Sources*, 2011, **196**(10), 4427–4435.
39 L. Klüpfel, M. Keiluweit, M. Kleber and M. Sander, Redox properties of plant biomass-derived black carbon (biochar), *Environ. Sci. Technol.*, 2014, **48**(10), 5601–5611.
40 J. M. Novak, I. Lima, J. W. Gaskin, C. Steiner, K. C. Das and M. Ahmedna, Characterization of designer biochar produced at different temperatures and their effects on a loamy sand, *Ann. Environ. Sci.*, 2009, **3**, 195–206.
41 J. E. Amonette and S. Joseph, Characteristics of biochar: microchemical properties, in *Biochar for Environmental Management*, Routledge, 2012, pp. 65–84.
42 D. Xin, M. Xian and P. C. Chiu, New methods for assessing electron storage capacity and redox reversibility of biochar, *Chemosphere*, 2019, **215**, 827–834.
43 J. Lehmann and S. Joseph, *Biochar for Environmental Management: Science, Technology and Implementation*. Routledge, 2015.
44 A. P. F. Maillard, J. C. Espeche, P. Maturana, A. C. Cutro and A. Hollmann, Zeta potential beyond materials science: Applications to bacterial systems and to the development of novel antimicrobials, *Biochim. Biophys. Acta, Biomembr.*, 2021, **1863**(6), 183597.
45 L. Riva, H. K. Nielsen, Ø. Skreiberg, L. Wang, P. Bartocci, M. Barbanera, *et al.*, Analysis of optimal temperature, pressure and binder quantity for the production of biocarbon pellet to be used as a substitute for coke, *Appl. Energy*, 2019, **256**, 113933.
46 L. Yu, Y. Wang, Y. Yuan, J. Tang and S. Zhou, Biochar as electron acceptor for microbial extracellular respiration, *Geomicrobiol. J.*, 2016, **33**(6), 530–536.

47 A. Tagliaferro, M. Rovere, E. Padovano, M. Bartoli and M. Giorcelli, Introducing the novel mixed Gaussian-Lorentzian lineshape in the analysis of the Raman signal of biochar, *Nanomaterials*, 2020, **10**(9), 1748.

48 Y. Zhang, X. Xu, L. Cao, Y. S. Ok and X. Cao, Characterization and quantification of electron donating capacity and its structure dependence in biochar derived from three waste biomasses, *Chemosphere*, 2018, **211**, 1073–1081.

49 R. Gabhi, L. Basile, D. W. Kirk, M. Giorcelli, A. Tagliaferro and C. Q. Jia, Electrical conductivity of wood biochar monoliths and its dependence on pyrolysis temperature, *Biochar*, 2020, **2**, 369–378.

50 C. I. Torres, A. K. Marcus, P. Parameswaran and B. E. Rittmann, Kinetic Experiments for Evaluating the Nernst–Monod Model for Anode-Respiring Bacteria (ARB) in a Biofilm Anode, *Environ. Sci. Technol.*, 2008, **42**(17), 6593–6597.

51 B. E. Logan, Scaling up microbial fuel cells and other bioelectrochemical systems, *Appl. Microbiol. Biotechnol.*, 2010, **85**(6), 1665–1671.

52 D. Surovtseva, E. Crossin, R. Pell and L. Stamford, Toward a life cycle inventory for graphite production, *J. Ind. Ecol.*, 2022, **26**(3), 964–979.

53 D. A. Notter, M. Gauch, R. Widmer, P. Wager, A. Stamp, R. Zah, *et al.*, *Contribution of Li-Ion Batteries to the Environmental Impact of Electric Vehicles*, 2010.

54 S. W. Gao, X. Z. Gong, Y. Liu, and Q. Q. Zhang, *Energy Consumption and Carbon Emission Analysis of Natural Graphite Anode Material for Lithium Batteries*, En Trans Tech Publ, 2018, pp. 985–990.

55 R. J. Saft, Life cycle assessment of a pyrolysis/gasification plant for hazardous paint waste, *Int. J. Life Cycle Assess.*, 2007, **12**(4), 230–238.

56 K. G. Roberts, B. A. Gloy, S. Joseph, N. R. Scott and J. Lehmann, Life cycle assessment of biochar systems: estimating the energetic, economic, and climate change potential, *Environ. Sci. Technol.*, 2010, **44**(2), 827–833.

57 N. A. Ryan, J. X. Johnson and G. A. Keoleian, Comparative assessment of models and methods to calculate grid electricity emissions, *Environ. Sci. Technol.*, 2016, **50**(17), 8937–8953.

58 G. W. Meetham, High-temperature materials—a general review, *J. Mater. Sci.*, 1991, **26**(4), 853–860.

59 S. Xia, H. Xiao, M. Liu, Y. Chen, H. Yang and H. Chen, Pyrolysis behavior and economics analysis of the biomass pyrolytic polygeneration of forest farming waste, *Bioresour. Technol.*, 2018, **270**, 189–197.

60 Y. Gao, X. Wang, Y. Chen, P. Li, H. Liu and H. Chen, Pyrolysis of rapeseed stalk: Influence of temperature on product characteristics and economic costs, *Energy*, 2017, **122**, 482–491.